PROCEEDINGS OF SPIE

SPIEDigitalLibrary.org/conference-proceedings-of-spie

Optical-resolution photoacoustic microscopy of amyloid-β deposits in vivo

Song Hu, Ping Yan, Konstantin Maslov, Jin-Moo Lee, Lihong V. Wang

Song Hu, Ping Yan, Konstantin Maslov, Jin-Moo Lee, Lihong V. Wang, "Optical-resolution photoacoustic microscopy of amyloid-β deposits in vivo," Proc. SPIE 7564, Photons Plus Ultrasound: Imaging and Sensing 2010, 75643D (23 February 2010); doi: 10.1117/12.843919

SPIE.

Event: SPIE BiOS, 2010, San Francisco, California, United States

Optical-resolution photoacoustic microscopy of amyloid-β deposits *in vivo*

Song Hu[1], Ping Yan[2], Konstantin Maslov[1], Jin-Moo Lee[2,*], and Lihong V. Wang[1,*]

[1]Optical Imaging Laboratory, Department of Biomedical Engineering, Washington University in St. Louis, St. Louis, Missouri, USA 63130
[2]Department of Neurology and the Hope Center for Neurological Disorders, Washington University School of Medicine, St. Louis, Missouri, USA 63110
*leejm@neuro.wustl.edu (animal model), and lhwang@biomed.wustl.edu (photoacoustics).

ABSTRACT

Advances in high-resolution imaging have permitted microscopic observations within the brains of living animals. Applied to Alzheimer's disease (AD) mouse models, multiphoton microscopy has opened a new window to study the real-time appearance and growth of amyloid plaques. Here, we report an alternative technology—optical-resolution photoacoustic microscopy (OR-PAM)—for *in vivo* imaging of amyloid plaques in a transgenic AD mouse model. *In vivo* validation using multiphoton microscopy shows that OR-PAM has sufficient sensitivity and spatial resolution to identify amyloid plaques in living brains. In addition, with dual-wavelength OR-PAM, the three-dimensional morphology of amyloid plaques and the surrounding microvasculature are imaged simultaneously through a cranial window. *In vivo* transcranial OR-PAM imaging of amyloid plaques is highly likely once the imaging parameters are optimized.

Keywords: Optical-resolution photoacoustic microscopy, Alzheimer's disease, amyloid-β, dual contrast.

1. INTRODUCTION

Amyloid-β is hypothesized to play a major role in the pathogenesis of Alzheimer's Disease (AD), but the underlying mechanisms are still elusive[1]. Intense interest has been generated by recent technological developments that have permitted noninvasive imaging of amyloid deposits in animal models or patients[2, 3]. In particular, positron emission tomography (PET) with a radiotracer, Pittsburgh compound B (PIB), promises to revolutionize the diagnosis and treatment of AD[4]. However, the neuropathologic changes in AD are microscopic[5], and subtle changes due to disease progression or treatment may be undetectable by PIB-PET because of its low spatial resolution. Multiphoton microscopy, a commercially available laser scanning microscopy technique, has been extremely useful for intravital brain imaging in AD mouse models, allowing imaging of amyloid plaques with high sensitivity and sub-micrometer resolution[6, 7]. However, the fluorescence signal declines quadratically with two-photon excitation, limiting its imaging depth to ~200 μm through thinned- or open-skull windows[8, 9]. These required invasive skull preparations limit imaging of the underlying brain to the narrow window, and there is some evidence that the window itself may alter the behavior of the underlying brain[10].

Optical-resolution photoacoustic microscopy (OR-PAM)[11], a newly developed optical absorption microscopy technique, has successfully demonstrated *in vivo* brain imaging with micrometer resolution through intact skulls of adult mice[12]. Microhemodynamic monitoring shows its high sensitivity and adequate temporal resolution[13], and functional chronic imaging demonstrates its potential in monitoring disease activity[14]. With the aid of amyloid-specific absorption contrast agents, OR-PAM is expected to visualize amyloid plaques *in vivo* with high spatial resolution.

Photons Plus Ultrasound: Imaging and Sensing 2010, edited by Alexander A. Oraevsky, Lihong V. Wang,
Proc. of SPIE Vol. 7564, 75643D · © 2010 SPIE · CCC code: 1605-7422/10/$18 · doi: 10.1117/12.843919

2. METHODS AND MATERIALS

2.1 OR-PAM system

For photoacoustic imaging[15], the tissue generally is irradiated by a short-pulsed laser beam, and ultrasonic waves (also called photoacoustic waves) are induced as a result of transient thermoelastic expansion due to the laser excitation. Since the generated photoacoustic signal is highly correlated with the local optical absorption, 3D distribution of endogenous and exogenous absorbers (such as hemoglobin and Congo red in this case, respectively) can be reconstructed based on the detected photoacoustic signal. To maximize the imaging sensitivity, optical illumination and ultrasonic detection in our OR-PAM system are configured confocally by an acoustic-optical beam splitter, which consists of two right-angle prisms and a thin silicone oil layer in between (Fig. 1). Although matching the prism glass in optical refractive index, the silicone oil has a large acoustic impedance mismatch with the glass. Thus, the beam splitter is nearly transparent to the optical illumination, but the oil-glass surface reflects almost all the ultrasonic signals to a 75 MHz ultrasonic transducer attached to the vertical side of the bottom prism. The near-diffraction-limited optical focusing achieved by a commercial microscope objective determines the lateral resolution of OR-PAM, which is 5 μm with the current configuration. An acoustic lens (NA: 0.46) is attached to the bottom of the beam splitter and immersed in a water tank to collect photoacoustic signals. A window is opened at the bottom of the water tank and sealed with an ultrasonically and optically transparent polyethylene membrane to expose the imaging site. For simplification, the water tank is not shown in Fig. 1. A detailed system description, however, can be referenced in our previous publications [11, 14, 16].

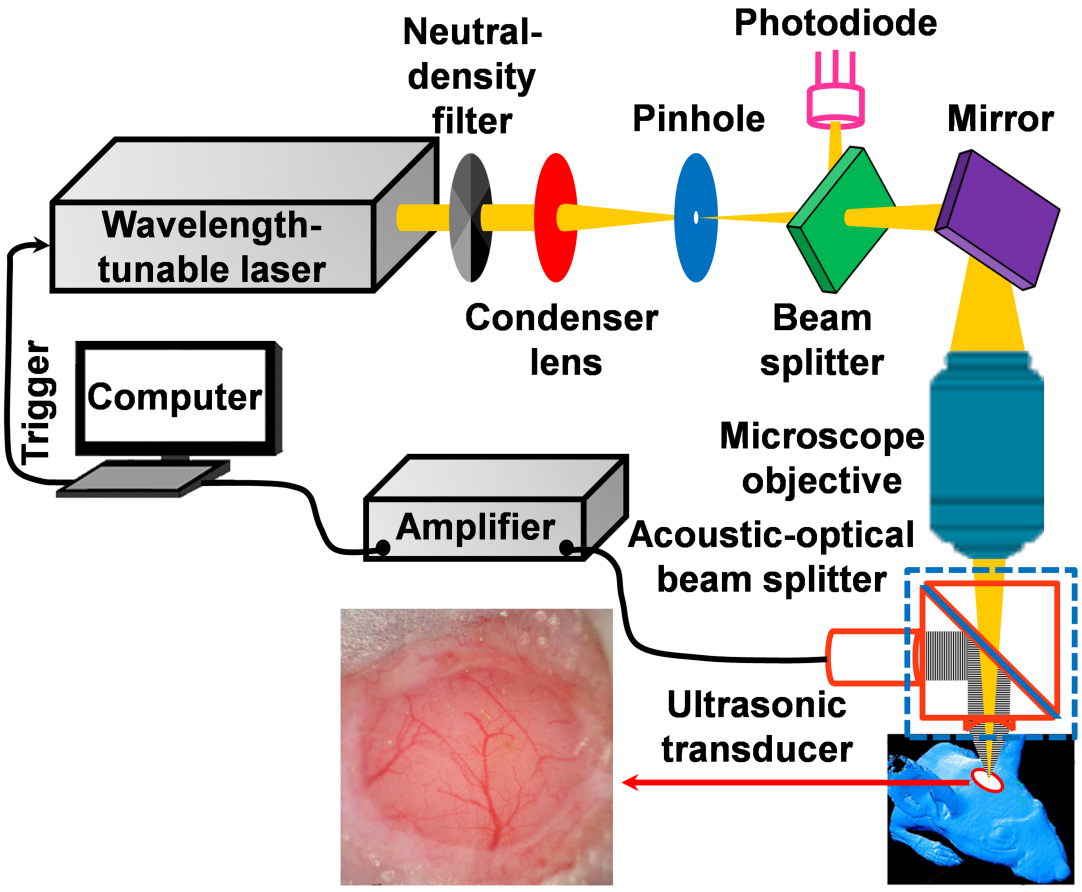

Figure 1. Schematic of the OR-PAM system.

2.2 Animal preparation

APPswe/PS1dE9 (APP/PS1) mice (The Jackson Laboratory, Bar Harbor, ME, USA) were used in this study. The production, genotyping, and background strains of these mice have been described previously[17]. All animal procedures

were carried out in compliance with the laboratory animal protocols approved by the School of Medicine Animal Studies Committee of Washington University in St. Louis.

For *in vivo* labeling, Congo red was injected into the cisterna magna of anesthetized APP/PS1 mice using a Hamilton syringe (20 µl, 30 gauge) guided by a micromanipulator under an operating microscope. A midline skin incision was made from the superior nuchal line to the level of the C3 vertebrae, followed by a strict midline blunt dissection of muscles. The syringe was backfilled with 15 µl Congo red (0.2% in ACSF, filtered through a 0.20-µm syringe filter). The atlanto-occipital membrane was quickly punctured immediately after it was exposed, and 10 µl Congo red solution was slowly infused into the cisterna magna with a picospritzer over 10 minutes; the needle was kept in place for another 10 minutes before the wound was closed. *In vivo* labeling of amyloid deposits was typically observed within 24 hours after injection. Before the OR-PAM experiment, the mouse was given an intraperitoneal injection of 87 mg/kg Ketamine and 13 mg/kg Xylazine for anesthesia, and was immobilized in a stereotaxic imaging stage. The plastic-covered cranial window was cleaned with saline, and ultrasonic gel was applied between the cranial window and the polyethylene membrane for effective acoustic coupling. Throughout the experiment, anesthesia was maintained by vaporized isoflurane (1.0-1.5% isoflurane with an airflow rate of 1 liter/min), and the body temperature of the mouse was maintained at 37ºC with a temperature controlled heating pad. At the end of the experiment, the cranial window was cleaned again with saline and the mouse was transferred to the multiphoton microscopy system.

3. RESULTS AND DISCUSSION

To examine the plaque imaging capability of OR-PAM in living mice, OR-PAM images were directly compared with the images acquired by multiphoton and conventional fluorescence microscopy. A 10-month-old APP/PS1 mouse was injected with Congo red through the cisterna magna to label amyloid plaques *in vivo*. Twenty-four hours after injection, an open-skull cranial window covered by a plastic coverslip was created over the parietal cortex. A region of interest containing a variety of amyloid plaques and blood vessels was selected for both OR-PAM imaging (Fig. 2A) and multiphoton microscopic imaging (Fig. 2B). Two optical wavelengths (523 nm and 570 nm) were used to differentiate Congo red contrast from endogenous hemoglobin contrast. In the processed dual-contrast OR-PAM image, plaques were pseudocolored blue and blood vessels were colored yellow. Images acquired using OR-PAM and multiphoton microscopy were directly compared, revealing excellent correlation in plaque distribution (arrows, Figs. 2A and 2B).

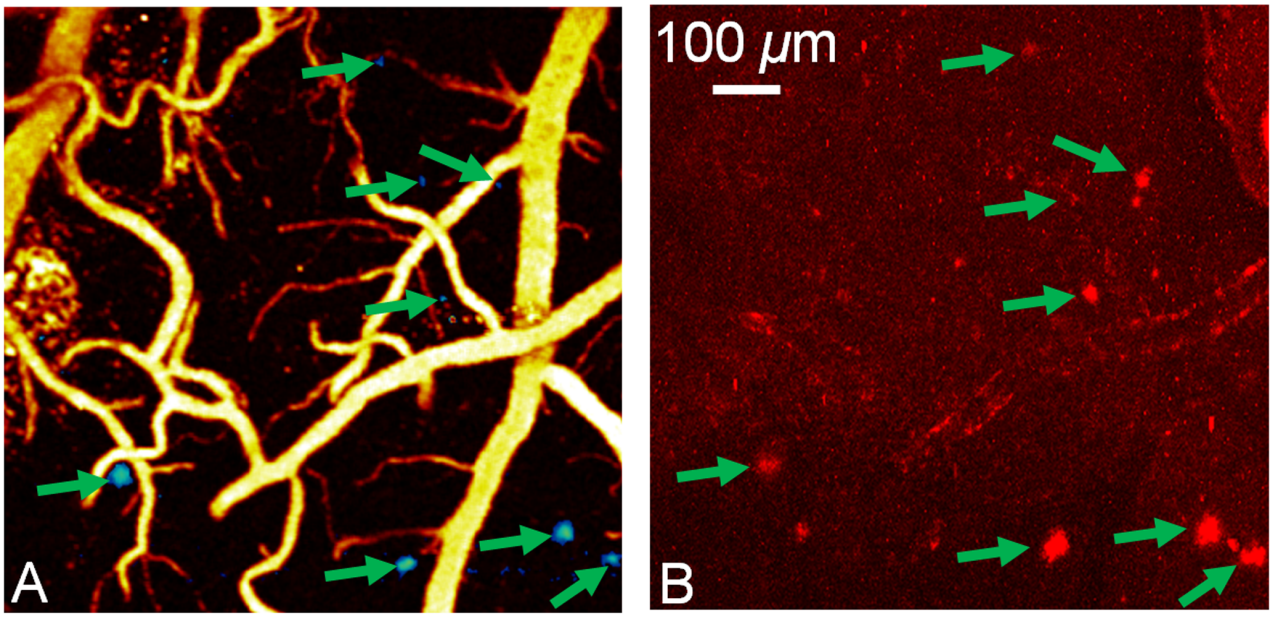

Figure 2. *In vivo* brain imaging of a Congo-red-injected 10-month-old APP/PS1 mouse through a cranial window. (A) Dual-contrast optical-resolution photoacoustic microscopic image, and (B) multiphoton image. Amyloid plaques are colored blue and blood vessels are colored yellow. Arrows: plaques. Scale bar in (B) applies for (A-B).

4. CONCLUSIONS

OR-PAM is capable of imaging single capillaries through intact mouse skulls. *In vivo* transcranial OR-PAM imaging of amyloid plaques, which are similar to or larger than capillaries, is highly likely by matching the excitation wavelengths with the absorption peaks of amyloid-specific dyes, and/or by enhancing the optical absorption of dyes.

ACKNOWLEDGEMENTS

This work was sponsored by National Institutes of Health grants R01 NS48283, R01 NS67905, P01 NS32636 (J ML), R01 EB000712, R01 NS46214, R01 EB008085, and U54 CA136398. LVW has a financial interest in Microphotoacoustics, Inc. and Endra, Inc., which, however, did not support this work.

REFERENCES

1. M. E. McLellan, S. T. Kajdasz, B. T. Hyman and B. J. Bacskai, "In vivo imaging of reactive oxygen species specifically associated with thioflavine S-positive amyloid plaques by multiphoton microscopy," *J Neurosci* **23**(6), 2212-2217 (2003)
2. R. J. Killiany, T. Gomez-Isla, M. Moss, R. Kikinis, T. Sandor, F. Jolesz, R. Tanzi, K. Jones, B. T. Hyman and M. S. Albert, "Use of structural magnetic resonance imaging to predict who will get Alzheimer's disease," *Annals of Neurology* **47**(4), 430-439 (2000)
3. A. Nordberg, "PET imaging of amyloid in Alzheimer's disease," *Lancet Neurology* **3**(9), 519-527 (2004)
4. W. E. Klunk, H. Engler, A. Nordberg, Y. Wang, G. Blomqvist, D. P. Holt, M. Bergstrom, I. Savitcheva, G. F. Huang, S. Estrada, B. Ausen, M. L. Debnath, J. Barletta, J. C. Price, J. Sandell, B. J. Lopresti, A. Wall, P. Koivisto, G. Antoni, C. A. Mathis and B. Langstrom, "Imaging brain amyloid in Alzheimer's disease with Pittsburgh Compound-B," *Ann Neurol* **55**(3), 306-319 (2004)
5. B. J. Bacskai, W. E. Klunk, C. A. Mathis and B. T. Hyman, "Imaging amyloid-beta deposits in vivo," *J Cereb Blood Flow Metab* **22**(9), 1035-1041 (2002)
6. M. E. McLellan, S. T. Kajdasz, B. T. Hyman and B. J. Bacskai, "In vivo imaging of reactive oxygen species specifically associated with thioflavine S-positive amyloid plaques by multiphoton microscopy," *Journal of Neuroscience* **23**(6), 2212-2217 (2003)
7. W. E. Klunk, B. J. Bacskai, C. A. Mathis, S. T. Kajdasz, M. E. McLellan, M. P. Frosch, M. L. Debnath, D. P. Holt, Y. Wang and B. T. Hyman, "Imaging Abeta plaques in living transgenic mice with multiphoton microscopy and methoxy-X04, a systemically administered Congo red derivative," *J Neuropathol Exp Neurol* **61**(9), 797-805 (2002)
8. J. Grutzendler, N. Kasthuri and W. B. Gan, "Long-term dendritic spine stability in the adult cortex," *Nature* **420**(6917), 812-816 (2002)
9. E. M. Robbins, R. A. Betensky, S. B. Domnitz, S. M. Purcell, M. Garcia-Alloza, C. Greenberg, G. W. Rebeck, B. T. Hyman, S. M. Greenberg, M. P. Frosch and B. J. Bacskai, "Kinetics of cerebral amyloid angiopathy progression in a transgenic mouse model of Alzheimer disease," *J Neurosci* **26**(2), 365-371 (2006)
10. H. T. Xu, F. Pan, G. Yang and W. B. Gan, "Choice of cranial window type for in vivo imaging affects dendritic spine turnover in the cortex," *Nat Neurosci* **10**(5), 549-551 (2007)
11. K. Maslov, H. F. Zhang, S. Hu and L. V. Wang, "Optical-resolution photoacoustic microscopy for in vivo imaging of single capillaries," *Opt Lett* **33**(9), 929-931 (2008)
12. S. Hu, K. Maslov, V. Tsytsarev and L. V. Wang, "Functional transcranial brain imaging by optical-resolution photoacoustic microscopy," *J. Biomed. Opt.* **14**(4), 040503 (2009)
13. S. Hu, K. Maslov and L. V. Wang, "Noninvasive label-free imaging of microhemodynamics by optical-resolution photoacoustic microscopy," *Opt Express* **17**(9), 7688-7693 (2009)
14. S. Hu, K. Maslov and L. V. Wang, "In vivo functional chronic imaging of a small animal model using optical-resolution photoacoustic microscopy," *Med Phys* **36**(6), 2320-2323 (2009)
15. L. V. Wang, "Tutorial on photoacoustic microscopy and computed tomography," *Ieee Journal of Selected Topics in Quantum Electronics* **14**(1), 171-179 (2008)
16. K. Maslov, H. F. Zhang, S. Hu and L. V. Wang, "Optical-resolution confocal photoacoustic microscopy," *Proc. SPIE* **6856**, 685611 (2008)
17. J. L. Jankowsky, H. H. Slunt, T. Ratovitski, N. A. Jenkins, N. G. Copeland and D. R. Borchelt, "Co-expression of multiple transgenes in mouse CNS: a comparison of strategies," *Biomol Eng* **17**(6), 157-165 (2001)